ChemComm

COMMUNICATION

Cite this: *Chem. Commun.*, 2018, **54**, 3294

Received 20th February 2018,
Accepted 28th February 2018

DOI: 10.1039/c8cc01458b

rsc.li/chemcomm

Inhibition of amyloid Aβ aggregation by high pressures or specific D-enantiomeric peptides†

Italo A. Cavini,[ab] Claudia E. Munte,[ab] Markus Beck Erlach,[b] Thomas van Groen,[c] Inga Kadish,[c] Tao Zhang,[de] Tamar Ziehm,[e] Luitgard Nagel-Steger,[de] Janine Kutzsche,[e] Werner Kremer,[b] Dieter Willbold[de] and Hans Robert Kalbitzer*[b]

Pressure can shift the polymer–monomer equilibrium of Aβ, increasing pressure first leads to a release of Aβ-monomers, surprisingly at pressures higher than 180 MPa repolymerization is induced. By high pressure NMR spectroscopy, differences of partial molar volumes ΔV^0 and compressibility factors $\Delta\beta'$ of polymerization were determined at different temperatures. The D-enantiomeric peptides RD2 and RD2D3 bind to monomeric Aβ with affinities substantially higher than those determined for fibril formation. By reducing the Aβ concentration below the critical concentration for polymerization they inhibit the formation of toxic oligomers. Chemical shift perturbation allows the identification of the binding sites. The D-peptides are candidates for drugs preventing Alzheimer's disease. We show that RD2D3 has a positive effect on the cognitive behaviour of transgenic (APPSwDI) mice prone to Alzheimer's disease. The heterodimer complexes have a smaller Stokes radius than Aβ alone indicating the recognition of a more compact conformation of Aβ identified by high pressure NMR before.

Alzheimer's disease (AD) is one of the most common and severe forms of dementia, but its complex pathogenesis is still not fully understood (for a review see ref. 1). A main histological feature of AD is the presence of amyloid plaques in the brains of patients, whose most abundant constituent is the β-amyloid protein (Aβ). According to the widely accepted amyloid hypothesis, Aβ aggregates are the primary cause of the disease.[2] Soluble monomeric Aβ is produced by a proteolytic cleavage of the amyloid precursor protein (APP). It can assemble into oligomers, that are assumed to be the primary toxic species,[3] and finally form the fibrils of amyloid plaques.

The peptide is usually assumed to adopt a predominantly unstructured conformation in solution that only transiently forms helical secondary structure elements.[4–6] However, also a compact structure of monomeric Aβ has been reported.[7] High pressure NMR spectroscopy revealed that monomeric Aβ exists in solution in an equilibrium of at least three different conformational states.[8] In contrast, the peptide has a cross-β conformation within the amyloid fibrils of the senile plaques and after polymerization *in vitro*.[9–11] The refolding of Aβ from a partially α-helical to a β-strand conformation is assumed to be a critical step in pathogenesis of AD.[12] The mechanism of this conversion is still unknown, its understanding is however crucial for the understanding of AD in general and the development of effective molecular therapies.

A number of different approaches to prevent or to cure Alzheimer's disease have been proposed in the past (for a review see *e.g.* ref. 13). An interesting development is the use of D-enantiomeric peptides found by mirror image phage display[14] that bind to Aβ-molecules. The dodecapeptide D3 orally administered to AD transgenic mice is able to reduce the plaque load and to increase the cognitive behavior.[15]

In this paper we will analyze for the first time the polymerization/depolymerization mechanism of Aβ-fibrils by high pressure NMR spectroscopy (HPNMR). This is crucial for understanding amyloid formation and the mode of action of two structurally not yet characterized D-enantiomeric peptides H-ptlhthnrrrrr-NH_2 (RD2) and H-ptlhthnrrrrrrprtrlhthrnr-NH_2 (RD2D3). These peptides are supposed to lead also to depolymerization of Aβ-polymers *in vitro* and *in vivo*. Besides NMR spectroscopy, surface plasmon resonance and analytical ultracentrifugation will be applied for analysis. We will also show that RD2D3 has a positive effect on the cognitive behavior of transgenic AD mice (APPSwDI).

The polymerization and depolymerization of Aβ are complicated reactions including a number of intermediate states. For their study the populations of these states can be reversibly

[a] *Physics Institute of São Carlos, University of São Paulo, São Carlos, SP, Brazil*
[b] *Institute of Biophysics and Physical Biochemistry, University of Regensburg, Universitätsstrasse 31, 93053 Regensburg, Germany. E-mail: hans-robert.kalbitzer@biologie.uni-regensburg.de*
[c] *University of Alabama at Birmingham, Birmingham, Alabama 35294, USA*
[d] *Heinrich-Heine University Düsseldorf, Institute for Physical Biology and BMFZ, 40225 Düsseldorf, Germany*
[e] *Institute of Complex Systems, Structural Biochemistry (ICS-6), Forschungszentrum Jülich GmbH, 52425 Jülich, Germany*

† Electronic supplementary information (ESI) available. See DOI: 10.1039/c8cc01458b

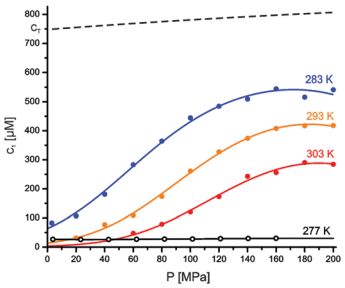

Fig. 1 Pressure induced depolymerization of Aβ. The equilibrium concentration c_1 of monomeric Aβ was plotted as function of pressure P and fitted with eqn (1). (closed circles) c_1 at a total Aβ concentration (c_T) of 750 μM at 0.1 MPa and (broken line) corrected for the pressure dependent compression of the solvent. (open circles) c_1 at c_T of 30 μM (for details see ESI†). Parameters obtained from the fit of the data are given in Table 1.

Table 1 Thermodynamics of polymerization[a]

T [K]	c_1/c_T (at 200 MPa)	K_D (at 0.1 MPa) [μM]	K_D (at 200 MPa) [mM]
283	0.70	88.3	2.7
293	0.55	14.6	1.5
303	0.38	2.8	0.7

T [K]	ΔG^0 [kJ mol^{-1}]	ΔV^0 [mL mol^{-1}]	$\Delta\beta^{0\prime}$ [mL MPa^{-1} mol^{-1}]
283	22.0 ± 0.3	−98 ± 6	−0.59 ± 0.05
293	27.1 ± 0.4	−125 ± 6	−0.69 ± 0.04
303	32.2 ± 1.0	−148 ± 15	−0.78 ± 0.10

[a] Data were obtained from the sample described in Fig. 1. c_1, concentration of monomeric Aβ, c_T, total concentration of Aβ (in monomeric units), T, K_D, ΔG^0, ΔV^0, $\Delta\beta^{0\prime}$, absolute temperature, dissociation constant of a monomer from polymers, differences of free energies, partial molar volumes and compressibility factors.

perturbed by pressure. After a rapid pressure jump of 40 MPa a dynamic equilibrium is typically obtained after two to three hours at 283 K (see Fig. S1, ESI†). After a rapid decrease of pressure the repolymerization requires more than 12 hours at 283 K for reaching equilibrium (data not shown).

It is generally accepted (see *e.g.* ref. 16) that NMR visible signals in solution essentially correspond to monomeric Aβ. Thus the NMR signal intensities can be directly used to determine the monomer concentration c_1 of the peptide dissolved in D_2O from one-dimensional spectra. Application of pressure leads to an increase of the NMR signal of the peptide indicating a depolymerization of Aβ polymers (Fig. 1). At approximately 200 MPa a plateau is reached and additional depolymerization does not occur at higher pressures. At 283 K, 23% of the peptide is still invisible (polymerized) at 200 MPa. The obtained maximum monomer level is strongly dependent on the temperature.

The simplest model[17] for a quantitative description assumes that the polymerization can be described by a single binding constant of the monomer to the polymer independent of the length of the polymer. We have derived a new expression (see ESI†) for fitting our high pressure NMR data:

$$c_1 = K_D\left(1 + \frac{K_D}{2c_T} - \sqrt{\frac{K_D^2}{4c_T^2} + \frac{K_D}{c_T}}\right) \quad (1)$$

From a fit of the data the dissociation constant K_D at pressure P, the volume difference after binding ΔV^0 and the compressibility factor difference $\Delta\beta^{0\prime}$ are obtained (Table 1) when the monomer concentration c_1 and total concentration c_T of Aβ are known. The negative $\Delta\beta'$ explains the saturation like behavior and predicts a repolymerization at very high pressures. Below a critical total concentration c_{CMC} defined by the K_D no (de)polymerization should occur as it is also observed experimentally at 60 μM Aβ (Fig. 1).

High pressures prefer structures with smaller partial molar volumes V. In most (but not all) cases, this leads to a dissociation of protein complexes as we can observe for Aβ(1–40) polymers. The differences in partial molar volumes between an Aβ-monomer free in solution and bound to fibrils is with −98 mL mol^{-1} at 283 K relatively large and further increases with temperature to −148 mL mol^{-1} at 303 K (Table 1). The corresponding differences in free energy ΔG at ambient pressure increase from 22.0 kJ mol^{-1} to 32.2 kJ mol^{-1} with temperature. The last value is close to 34.7 kJ mol^{-1} determined by Wulff *et al.*[18] for monomer association by gel electrophoresis. The K_D-value is strongly dependent on the pressure and significantly increases with temperature. At 303 K the K_D-value is increased more than 30 fold. However, the dissociation process does not increase further at approximately 200 MPa but a saturation-like behavior is observed (Fig. 1). This is a consequence of the smaller compressibility of Aβ when bound to fibrils. In contrary, the negative difference of the partial molar compressibility factor $\Delta\beta^{0\prime}$ predicts a reformation of fibrils at higher pressures. As proposed earlier by us[8] the reduction of the monomer affinity by pressure could at least partly depend on a pressure dependent shift of the equilibrium between an Aβ-conformer able to directly interact with the fibrils and a conformer that first binds unspecifically to the fibrils before finding its correct cross-beta conformation. Here conformational state 1 would be a candidate for a cross-beta like conformation and conformational state 2 for a weakly interacting, more disordered conformation since its relative population is inverted relative to that of state 2 at higher pressures. The strong reduction of the Aβ partial molar volume by 98 mL mol^{-1} after binding is relatively large compared to other amyloid forming proteins. For lysozyme deficient in SS-bonds[19] it is only 53 mL mol^{-1}. The volume difference of 43 mL mol^{-1} for the transition between state 1 and 2 could explain the difference.

An interesting development in fighting Alzheimer's disease is the use of D-enantiomeric peptides.[15] The molecular mechanism remains still to be elucidated. We studied here the interaction of Aβ with the D-enantiomeric peptides RD2 and RD2D3, derivatives of D3 with similar properties. The published experimental data focused mainly on conditions where a mixture of Aβ-oligomers and fibrils coexists. In this paper, we concentrate on the interaction of the D-peptides with Aβ monomers and therefore performed all NMR experiments at Aβ concentrations that at a given temperature are below the critical concentration c_{CMC} for polymerization (Table 1).

At low relative concentrations of the D-peptides the peak intensities of non-exchangeable protons in the 1D spectra and

the amide cross peak volumes decrease only moderately allowing the direct observation of signal changes by solution NMR. At high relative concentrations of the D-peptides the NMR signal is strongly reduced. Here, the formation of large complexes between Aβ and the D-peptides with line widths too large to be observable seems to be a likely mechanism. Such complexes were already observed by electron microscopy (see *e.g.* ref. 15).

The K_D of RD2D3 from monomeric Aβ(1–42) was determined as 486 ± 69 nM at 298 K by surface plasmon resonance (Fig. S2, ESI†). After addition of RD2D3 to a solution of monomeric Aβ at 277 K, chemical shift and cross peak volume changes of the amide resonances of Aβ can be observed as to be expected when the peptides bind to Aβ monomers (Fig. 2). The pH-value was carefully controlled (and corrected when necessary) by using the Tris chemical shift. A general reduction of the average cross peak volumes by approximately 15% is observed as to be expected for an increase of the rotational correlation time by binding of RD2D3 to Aβ in a molar ratio of 0.2. The putative interaction sites of RD2D3 with Aβ are highlighted on different 3D-structures available (Fig. 2). At higher relative concentrations of RD2 or RD2D3 the sharp NMR signals from free Aβ are strongly quenched indicating the formation of large heteropolymers. The intensity reduction of the NMR signals provides an indirect possibility to quantify their concentrations. The concentrations of the free peptides and the heterodimers easily can be determined from characteristic, superposition free signals in the 1D-spectra (see ESI†). At high concentrations of the D-peptides only a broad peak remains of the heterodimer (Fig. 3A and B). When the concentration of the D-peptides is increased the concentration of free Aβ is strongly reduced and levels off almost to zero at relative concentrations larger than 1 (Fig. 3). Simultaneously, the concentrations of the presumed Aβ-D-peptide heterodimers first increase and then stay constant at a concentration of about 15 μM (Fig. 3C). In parallel to the formation of the heterodimers the spectral intensity of visible Aβ NMR signal decreases. Such a behavior would be expected when the heterodimer concentrations are higher than the critical concentration of approximately 15 μM for the formation of large heteropolymers.

The size of the heterodimers can be determined by diffusion NMR measurements (Fig. 3D). Unexpectedly, for free Aβ a hydrodynamic (Stokes) radius r_H of 1.58 ± 0.06 nm is obtained. In the presence of D-peptides the diffusion curve is shifted to smaller gradient values indicating a smaller hydrodynamic radius. When only the broad signal from methyl groups in

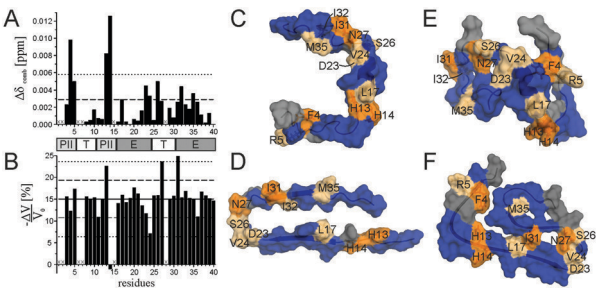

Fig. 2 The interaction sites of RD2D3 with Aβ(1–40). (left) The sample contained 60 μM ^{15}N-labeled Aβ(1–40) and 12 μM RD2D3. For details see ESI.† (A) Plot of the combined chemical shift changes $\Delta\delta_{comb}$ of the backbone amide protons and nitrogens *versus* the sequence position when RD2D3 is added. Broken line, σ_0; pointed line, $2\sigma_0$. The bar represents a secondary structure propensities of Aβ(1–40) in solution proposed by Danielsson *et al.*[6] PII: polyproline II like helix, T: turn or hinge region, E: extended strand. (B) Plot of the average cross peak volume changes $-\Delta V/V_0$ after addition of RD2D3. Solid line, mean; broken line, mean ± σ; pointed line, mean ± 2σ. Residues not detected in the [^{1}H,^{15}N]-HSQC spectrum are labelled with "X". The significant cross peak volume $-\Delta V/V_0$ and chemical shift changes $\Delta\delta_{comb}$ induced by the interaction with RD2D3 are plotted on (C) the NMR solution structure reported by Watson *et al.*,[20] (D) on the cross beta structure of a monomeric unit of a fibril from solid state NMR,[9] (E) on the NMR structure reported by Vivekanandan *et al.*[7] and (F) on the Aβ(1–42) cryoelectron microscopy fibril structure.[11] (light orange) Residues with chemical shift changes $>\sigma_0$ but $\leq 2\sigma_0$ and/or cross peak volume changes $>\langle -\Delta V/V_0\rangle + \sigma_0$ but $\leq\langle -\Delta V/V_0\rangle + 2\sigma_0$, (dark orange) residues with chemical shift changes $>2\sigma_0$ and/or cross peak volume changes $>\langle -\Delta V/V_0\rangle + 2\sigma_0$, (gray) residues that could not clearly followed in the titration series, (blue) residues not showing significant interactions.

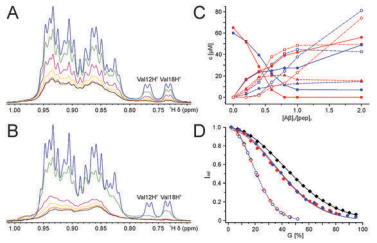

Fig. 3 Binding of RD2 and RD2D3 to Aβ. The samples contained 60 μM (RD2 titration) and 65 μM Aβ(1–40) (RD2D3 titration), respectively. The D-peptide concentration was varied by mixing with solutions containing Aβ and D-peptides (experimental details see ESI†). Part of a 800 MHz 1D NMR spectrum of Aβ with (A) RD2 and (B) RD2D3, respectively. Molar ratios of Aβ : RD2 or RD2D3 (blue) 1 : 0; (green) 1 : 0.4; (purple) 1 : 0.6; (yellow) 1 : 0.8; (orange) 1 : 1; (black) 1 : 2. (C) Concentrations c of different complexes as a function of the ratio of the total concentrations of RD2 and RD2D3 $[pep]_T$ to the total concentration $[A\beta]_T$ of Aβ, respectively. Titration with RD2 (blue), with RD2D3 (red). (filled squares) Free Aβ, (filled triangles) Aβ-D-peptide dimer, (open squares) Aβ in large Aβ-D-peptide oligomers, (filled circles) free D-peptides and Aβ-D-peptide dimers, (open circles) D-peptides in large Aβ-D-peptide oligomers. (D) NMR diffusion measurements on free Aβ (black diamonds), Aβ–RD2 (blue circles) and Aβ–RD2D3 (red circles). Open symbols: signal of Tris-d_{11}. Relative concentrations of RD2D3 and RD2 to Aβ 1 : 0.6 and 1 : 2, respectively. The relative peak intensity I_{rel} was plotted as a function of the gradient strength G. Temperature, 283 K.

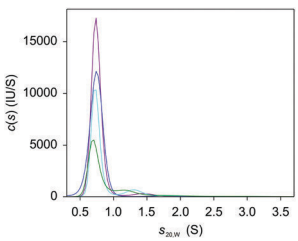

Fig. 4 Analytical ultracentrifugation of Aβ(1–40) in the presence of RD2D3. Sedimentation coefficient distributions $c(s)$ of 1 μM FITC–Aβ(1–40) alone (purple) and incubated with 1 μM (blue), 5 μM (cyan) and 20 μM RD2D3 (green) calculated from the sedimentation velocity analysis (60 000 rpm, 283 K for 15 h).

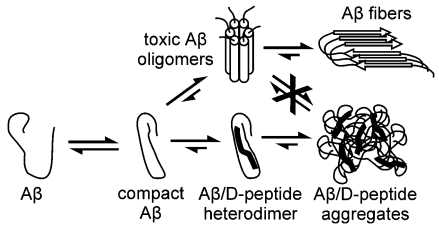

Fig. 5 Depolymerization and inhibition mechanism of D-peptides. RD2 and RD2D3 recognize a compact Aβ state leading to aggregates that are not able to form toxic oligomers.

the range between 0.8 ppm and 1 ppm is evaluated, that originates most likely from an Aβ-heterodimer, Stokes radii of 1.12 ± 0.04 and 1.14 ± 0.04 nm in the presence of RD2D3 and RD2, respectively, are obtained. At high concentrations of RD2D3 the cross peak intensities in the [^{1}H,^{15}N]-HSQC-spectra of Aβ decrease dramatically, since large polymers form that are not NMR visible (Fig. S3, ESI†) but in addition several weak new cross peaks appear that are typical for a second conformation of Aβ in slow exchange with free Aβ (green cross peaks Fig. S3, ESI†). From their similarity in chemical shifts to free Aβ they can tentatively be assigned to Ile31, Ile32, Val39, and Val40.

Analytical ultracentrifugation experiments have been carried out at a concentration of Aβ below its critical concentration (Table 1) at different RD2D3 concentrations (Fig. 4). In the absence of RD2D3 an *s*-value of 0.74 S was observed corresponding to a hydrodynamic radius of 1.55 nm, in line with our diffusion NMR experiments. The major peak shifted towards smaller *s*-values with increasing RD2D3 concentration. In addition, a new species is emerging when RD2D3 is present within 1–1.5 S. The average *s*-value of 1.24 S for a 1 : 1 RD2D3–Aβ complex with a molar mass of 7972 g mol^{-1} would correspond to a hydrodynamic radius of 1.54 nm.

The positive effects of the D-enantiomeric peptides D3 and RD2 on the development of Alzheimer's disease in mice has been shown already.[15,21] For the variant RD2D3 the *in vivo* effects are not studied yet. We treated transgenic APPSwDI mice intraperitoneal for 4 weeks with 8 mg kg^{-1} day^{-1} of RD2D3 using Alzet micropumps. We used the Morris water maze (MWM) test as test of spatial learning and memory performance for rodents. The treatment with RD2D3 significantly improved the cognitive performance of the animals and the long-term memory (Fig. S4, ESI†). The open field test showed that RD2D3 had no influence on the general behavior of tg-APPSwDI mice (Fig. S5, ESI†).

Concluding, we were able to show that β-amyloid can be reversibly depolymerized by high hydrostatic pressures. At pressures higher than 180 MPa repolymerization occurs. The inhibition mechanism is described in Fig. 5. The D-peptides recognize a more compact conformation of monomeric Aβ and form a heterodimer with a decreased Stokes radius. Although none of the published 3D-structures can explain the interaction sites identified perfectly, the interaction sites can be used to optimize the design of new inhibitors in future. Since the affinity of Aβ monomers to D-peptides is higher than that to amyloid fibrils, the free, polymerization prone Aβ-conformer is reduced below the critical concentration for polymerization (Table 1). The heterodimer then forms large aggregates causing a further quasi-irreversible reduction of free fibrillation leading to a destruction of toxic oligomers and amyloid fibrils in thermodynamic equilibrium.

This work was supported by the DFG (FOR 1997), the Humboldt Society, HFSPO, FCI, FAPESP (2010/01362-5, 2013/04433-9), the HGF HVF and Portfolio. The authors declare no competing financial interests. The experiments were conducted in accordance with the University of Alabama at Birmingham Institutional Animal Care and Use Committee (IACUC) guidelines, permit number 09457.

Conflicts of interest

There are no conflicts to declare.

Notes and references

1 M. P. Mattson, *Nature*, 2004, **430**, 631–639.
2 D. J. Selkoe and J. Hardy, *EMBO Mol. Med.*, 2016, **8**, 595–608.
3 I. Benilova, E. Karran and B. De Strooper, *Nat. Neurosci.*, 2012, **15**, 349–357.
4 R. Riek, P. Güntert, H. Döbeli, B. Wipf and K. Wüthrich, *Eur. J. Biochem.*, 2001, **268**, 5930–5936.
5 L. Hou, H. Shao, Y. Zhang, H. Li, N. K. Menon, E. B. Neuhaus, J. M. Brewer, I.-J. L. Byeon, D. G. Ray and M. P. Vitek, *J. Am. Chem. Soc.*, 2004, **126**, 1992–2005.
6 J. Danielsson, A. Andersson, J. Jarvet and A. Gräslund, *Magn. Reson. Chem.*, 2006, **44**, S114–S121.
7 S. Vivekanandan, J. R. Brender, S. Y. Lee and A. Ramamoorthy, *Biochem. Biophys. Res. Commun.*, 2011, **411**, 312–316.
8 C. E. Munte, M. Beck Erlach, W. Kremer, J. Koehler and H. R. Kalbitzer, *Angew. Chem., Int. Ed.*, 2013, **52**, 8943–8947.
9 T. Petkova, W.-M. Yau and R. Tycko, *Biochemistry*, 2006, **45**, 498–512.
10 T. Lührs, C. Ritter, M. Adrian, D. Riek-Loher, B. Bohrmann, H. Döbeli, D. Schubert and R. Riek, *Proc. Natl. Acad. Sci. U. S. A.*, 2005, **102**, 17342–17347.
11 L. Gremer, D. Schölzel, C. Schenk, E. Reinartz, J. Labahn, R. B. G. Ravelli, M. Tusche, C. Lopez-Iglesias, W. Hoyer and H. Heise, *Science*, 2017, **358**, 116–119.
12 M. Gross, *Curr. Protein Pept. Sci.*, 2000, **1**, 339–347.
13 X. Sun, L. Jin and P. Ling, *Drug Discoveries Ther.*, 2012, **6**, 285–290.
14 T. van Groen, I. Kadish, S. A. Funke, D. Bartnik and D. Willbold, *J. Alzheimer's Dis.*, 2013, **34**, 609–620.
15 S. A. Funke, T. van Groen, I. Kadish, D. Bartnik, L. Nagel-Steger, O. Brener, T. Sehl, R. Batra-Safferling, C. Moriscot and G. Schoehn, *ACS Chem. Neurosci.*, 2010, **1**, 639–648.
16 N. L. Fawzi, J. Ying, R. Ghirlando, D. A. Torchia and G. M. Clore, *Nature*, 2011, **480**, 268–272.
17 F. Oosawa, *J. Theor. Biol.*, 1970, **27**, 69–86.
18 M. Wulff, M. Baumann, A. Thümmler, J. K. Yadav, L. Heinrich, U. Knüpfer, D. Schlenzig, A. Schierhorn, J. U. Rahfeld and U. Horn, *Angew. Chem., Int. Ed.*, 2016, **55**, 5081–5084.
19 Y. O. Kamatari, S. Yokoyama, H. Tachibana and K. Akasaka, *J. Mol. Biol.*, 2005, **349**, 916–921.
20 A. A. Watson, D. P. Fairlie and D. J. Craik, *Biochemistry*, 1998, **37**, 12700–12706.
21 T. Groen, S. Schemmert, O. Brener, L. Gremer, T. Ziehm, M. Tusche, L. Nagel-Steger, I. Kadish, E. Schartmann and A. Elfgen, *Sci. Rep.*, 2017, **7**, 16275.

Supplementary Information

Inhibition of Amyloid Aβ Aggregation by High Pressures or Specific D-Enantiomeric Peptides

Italo A. Cavini[a,b], Claudia E. Munte[a], Markus Beck Erlach[b], Thomas van Groen[c], Inga Kadish[c], Tao Zhang[d,e], Tamar Ziehm[e], Luitgard Nagel-Steger[d,e], Janine Kutzsche[e], Werner Kremer[b], Dieter Willbold[d,e] and Hans Robert Kalbitzer[*,b]

[a] *Physics Institute of São Carlos, University of São Paulo, São Carlos, SP, Brazil*
[b] *Institute of Biophysics and Physical Biochemistry, University of Regensburg, Universitätsstrasse 31, 93053 Regensburg, Germany*
[c] *University of Alabama at Birmingham, Birmingham, Alabama 35294, USA*
[d] *Heinrich-Heine University Düsseldorf, Institute for Physical Biology and BMFZ, 40225, Düsseldorf, Germany*
[e] *Institute of Complex Systems, Structural Biochemistry, (ICS-6), Forschungszentrum Jülich GmbH, 52425 Jülich, Germany*

Table of Contents

Experimental Procedures

Materials

Uniformly ^{15}N-labelled, ^{13}C, ^{15}N-labelled and unlabelled Aβ(1-40) (4329.9 Da) was purchased from rPeptide (Bogard, Georgia, U.S.A.). Residues 1 - 40 of Aβ(1-40) correspond to residues 672 - 711 of βAPP770 (UniProtKB entry P05067). EDTA-d_{16} and Tris-d_{11} were purchased from Cambridge Isotope Laboratories (Andover, Massachusetts, U.S.A.). RD2 and RD2D3 are D-enantiomeric peptides with the amino acid sequences ptlht hnrrr rr-NH_2 (1598.86 Da) and ptlht hnrrr rrrpr trlht hrnr-NH_2 (3180.69 Da), respectively. The peptides were purchased as reversed phase high performance liquid chromatography purified products (P&E, Potsdam Germany).

Sample preparation

All NMR samples were pre-treated with hexafluoro-2-propanol (HFIP) for producing uniform, unaggregated Aβ(1-40) peptide.[1] Details of the procedure are described by Munte et al..[2] For removing higher aggregates some samples were centrifuged at 50,000 g for 3 h at 277 K and only the supernatant was used for NMR spectroscopy. The samples used in Fig. 1 contained 750 µM Aβ(1-40) dissolved in buffer A in 99.5% ^2H_2O or 60 µM ^{15}N-labeled Aβ(1-40) dissolved in buffer A in 92% ^1H_2O / 8% ^2H_2O. The sample used for the titration with RD2D3 (Fig. 2) contained 60 µM ^{15}N-labeled Aβ(1-40) dissolved in 50 mM Tris-d_{11}, pH 7.00, 90 mM NaCl, 0.5 mM EDTA-d_{16}, 0.2 mM dioxane and 1 mM NaN_3, 50 µM DSS) in 92% ^1H_2O / 8% ^2H_2O and 12 µM RD2D3. The pH of samples was controlled by measuring the chemical shifts of Tris-d_{11} signals. It was adjusted for the Aβ-RD2D3 sample by addition of small amounts of DCl or NaOD until the chemical shift of the Tris-d_{11} signal corresponded to the sample in absence of RD2D3. The Aβ-concentration in both samples was identical.

The samples used in Fig. 3 contained 60 µM (titration with RD2) and 65 µM Aβ(1-40) (titration with RD2D3), respectively, dissolved in 50 mM Tris-d_{11}, pH 7.00, 90 mM NaCl, 0.5 mM EDTA-d_{16}, 0.2 mM dioxane and 1 mM NaN_3, 50 µM DSS) in 92% ^1H_2O / 8% ^2H_2O. Concentration of the samples used for the titration study with the D-enantiomeric peptides contained 60 µM ^{15}N-labeled Aβ(1-40) dissolved in buffer A in 92% ^1H_2O / 8% ^2H_2O (sample C). A sample D was prepared by addition of a solution of 5 mM RD2D3 to sample C, resulting in a final concentration of 240 µM RD2D3, respectively. The pH of samples was controlled by measuring the chemical shifts of Tris-d_{11} signals. It was adjusted for sample D by addition of small amounts of DCl or NaOD till the chemical shift of the Tris-d_{11} signal corresponded to that of sample C. Different peptide concentrations were obtained by mixing sample C with appropriate quantities of sample D.

NMR spectroscopy

All NMR spectra were recorded with Bruker Avance 800 NMR spectrometer operating at a ^{1}H frequency of 800.20 MHz. Measurements were performed in a 5 mm TCI cryo probe. The absolute temperature inside the probe heads was calibrated by measuring the chemical shift difference $\Delta\delta$ between the methyl and hydroxyl resonance of 100% methanol.[3] For the assignment of the chemical shifts of Aβ(1-40) 2D-TOCSY (55 ms mixing time), 2D-NOESY (200 ms mixing time) and [^{1}H-^{15}N]-HSQC spectra were recorded at 278 K, pH 7.1. ^{1}H-NMR shifts were referenced to DSS used as internal standard (0 ppm) or to perdeutero Tris-d_{11} whose

pressure and temperature dependent shifts have been mapped before. ^{15}N and ^{13}C chemical shifts were indirectly referenced to DSS according to Wishart et al.[4]. More stable values are obtained using amino acid specific combined chemical shifts $\Delta\delta_{comb}$.[5] Because of the required additivity of the chemical shifts the Hamming distance has been used in these calculations.

High pressure NMR experiments

High pressure NMR experiments were performed in a home-built on-line pressure system as described earlier by Arnold et al. 2002.[6] Pressure was applied to the NMR sample via pressurized fluids (methylcyclohexane or water) contained in high pressure lines (High Pressure Equipment Company, Linden, PA, USA). For generating the pressure a manually operated piston compressor and an air-to-liquid pressure intensifier (Barocycler®, HUB440, Pressure BioSciences Inc., South Easton, MA, USA), which is controlled by the spectrometer, were used. For the polymerization experiments at high Aβ concentrations pressure produced by a homemade manually operated piston compressor was transmitted via a high pressure line by methyl cyclohexane to borosilicate or quartz capillaries with an outer diameter of 3.8 to 4.0 mm and an inner diameter of 1 mm. Alternatively, for the experiments at low Aβ concentrations, pressure was transmitted by water to the high pressure ceramic cell (with an outer diameter of 5 mm and an inner diameter of 3 mm) from Daedalus Innovations LLC (Aston. PA. USA). A PET (polyethylene terephthalate) membrane acts as a flexible separator between the pressure fluid and the aqueous sample. To reduce the volume of the ceramic cell, a cylindric PEEK (polyether ether ketone) displacement body was used. A titanium autoclave connects the ceramic cell with the closed pressure line.

Determination of Stokes radii by NMR

Translational diffusion measurements were acquired with a modified pulsed field gradient stimulated echo sequence (PFGSTE)[7] including bipolar pulses[8] as One-Shot PFGSTE[9] on the same samples used in the other experiments shown in figure 3. The intensity I_x of a signal or a group of signals of compound x is dependent on its translational diffusion coefficient D_x, the gradient strength G (in percent of the maximum field strength) and a parameter α that describes the pulse sequence used, the length and absolute maximum strength of gradients and length of different delays (eq. S1a). Usually the signal $I_x(0)$ at gradient strength 0 is perturbed by artifacts and the intensity value $I_x(G = a)$ at a small gradient strength a (in this paper 2%) is taken for scaling and $I_{rel} = I_x/I_x(a)$ is plotted as a function of G. I_{rel} can be fitted by eq. S1b with α a global fit parameter and $C_x = I_x(0)/I_x(a)$ and D_x parameters characteristic for compound x.

$$I_x(G) = I_x(0)\, e^{-\alpha D_x G^2} \quad \text{(S1a)}$$

$$I_{x,rel} = C_x(a)\, e^{-\alpha D_x G^2} \quad \text{(S1b)}$$

The Stokes radius r_x of compound x is defined by

$$D_x = \frac{k_B \cdot T}{6\pi \cdot \eta \cdot r_x} \quad \text{(S2)}$$

with k_B the Boltzmann constant, η the viscosity of the solution and T is the absolute temperature. The Stokes radius r_x for a compound x and can be calculated from the Stokes radius r_y of a compound y as

$$r_x = r_y \frac{D_y}{D_x} \quad \text{(S3)}$$

In the calculations we used a hydrodynamic radius r_H of 0.307 nm for Tris[10] that was contained in the sample.

Quantification of data

For quantitative experiments 90-degree pulses and a repetition time of 13 s was used that is larger than 5-times the T_1-values of the compounds under investigation. The T_1-times of the relevant components were determined by inversion recovery experiments. At 277 K the T_1-times of the methyl groups of DSS, Tris and the H^δ resonances of the tyrosine and histidine residues of free Aβ were 1.4 s, 1.1 s, and < 0.8 s, respectively. When the sample contains as reference DSS, the DSS signal intensity increases with pressure more strongly than expected from the compression of the solvent alone. This is in agreement with the observation that DSS interacts with Aβ-aggregates.[11] Consequentially, it cannot be used as an internal standard for the concentration determination of Aβ. Therefore quantification of NMR-visible resonances was performed by using the residual perdeuterated signal of Tris-d_{11} added to the sample with a known concentration. The degree of perdeuteration of Tris-d_{11} was determined as 99.31 ± 0.03% from the integrals of the corresponding methyl resonances.

Analysis of the polymerization reaction

The pressure dependence of the Gibbs free energy ΔG_{1i} is given[12] as

$$\Delta G_{1i}(T,P) = \Delta G^0_{1i}(T_0,P_0) + \Delta V^0_{1i}(P-P_0) - \frac{\Delta\beta^{0\prime}_{1i}}{2}(P-P_0)^2 \quad \textit{(S4)}$$

where ΔV^0_{1i} and $\Delta\beta^{0\prime}_{1i}$ are the differences of the partial molar volumes and of the partial molar compressibility factors between state 1 and state i at temperature T_0 and pressure P_0, respectively. When the total concentration c_T of monomeric units is larger than the dissociation constant K_D of a monomeric unit M from the polymer P, the concentration of the free monomer c_1 is given by[13]

$$c_1 = K_D = e^{-\frac{\Delta G}{RT}} \quad \textit{(S5)}$$

If the condition $c_1 < K_D$ holds, for a linear polymer with a maximum chain length N, c_1 can be described by

$$c_1 = \frac{c_T(1-c_1/K_D)^2}{N(c_1/K_D)^{N+1} - (N+1)(c_1/K_D)^N + 1} \quad \textit{(S6)}$$

For large chain lengths, c_1 can be approximated by

$$c_1 = c_T \left(1 - \frac{c_1}{K_D}\right)^2 \qquad (S7)$$

Equation S7 has two solutions but only one solution is physically meaningful

$$c_1 = K_D \left(1 + \frac{K_D}{2\,c_T} - \sqrt{\frac{{K_D}^2}{4\,{c_T}^2} + \frac{K_D}{c_T}}\right) \qquad (S8)$$

Note that in a high pressure experiment the change of the total concentration with pressure has to be taken into account because of the compressibility of the solvent. The dependence of the dissociation constant of the monomer from the polymer on pressure can again be described by equation S4.

Assuming (in agreement with the literature) that in a good approximation only monomeric Aβ is visible in the solution NMR spectra, the concentration c_1 of the monomers can be obtained from the integrals of the resonance lines when an internal standard with known concentration is available (in our case Tris). The concentration c_1 is then given by

$$c_1 = \; c_R \frac{V_i}{V_R} \qquad (S9)$$

with c_R the concentration of the reference (that has to be corrected in high pressure NMR spectroscopy for the compression of the solvent), V_R the integral of the corresponding signal in the 1D or 2D spectrum, and V_i the integral of a given atom in amino acid *i* in the 1D spectrum or a cross peak of the amino acid *i* in the HSQC spectrum. The quantification of the NMR visible peptide was performed by comparing the integrals of non-exchangeable protons the H^{ε}-resonance line of Tyr10 and the $H^{\varepsilon 1}$-resonances of His6, His13, and His14 with the signal of the Tris buffer with known concentration.

Sedimentation velocity analysis

Sedimentation velocity (SV) analysis was carried out to determine the size distributions of Aβ(1-40) peptides in the presence or absence of RD2D3. All experiments were performed using a Beckman Optima XL-A ultracentrifuge (Beckman-Coulter, Brea, CA, USA), equipped with a fluorescence detection system[14] (Aviv, Lakewood, NJ, USA) and a four-hole rotor. Fluorescein isothiocyanate (FITC) labelled Aβ(1-40) peptides were commercially available (Catalog No. H-6326, Bachem, Bubendorf, Switzerland) and the fluorophore was connected to the additional alanine at the N-terminus of Aβ(1-40) (hereafter referred to as FITC-Aβ(1-40)). Peptide purity determined by HPLC was 92.4% according to the manufacturer. RD2D3 was synthesized and purchased from peptides & elephants GmbH (Potsdam, Germany). FITC-Aβ(1-40) was first dissolved in 1,1,1,3,3,3-hexafluoro-2-propanol and divided into small aliquots. All aliquots were then lyophilized and stored at -80 °C before use. For improved dissolution FITC-Aβ(1-40) was predissolved in 6 µl 10 mM NaOH before adding buffer containing 50 mM Tris, 90 mM NaCl, 0.5 mM EDTA and 0.01% Tween-20. The working concentration of FITC-Aβ(1-40) was 1 µM. RD2D3 stock solution was added into FITC-Aβ(1-40) solutions

accordingly to get final concentrations of 0 µM, 1 µM, 5 µM and 20 µM. The final volume for each sample was 110 µl. For AUC measurement 100 µl samples were loaded into 3 mm titanium double sector cells with quartz glass windows. After 3.5 h incubation at 10 °C in the machine all samples were centrifuged at 60,000 rpm (~257,000g) at 10 °C for 15 h. Note that pH values for all samples were maintained at 7.0 during sample preparation and ultracentrifugation. The software package Sedfit (Version 15.01b) was used to analyze all the datasets[15]. In detail, continuous distribution *c*(*s*) Lamm equation model[16] was applied to evaluate size distributions of samples treated with or without RD2D3. Fitting parameters including buffer density and viscosity were calculated using Sednterp (Version 20130813 BETA).[17] The partial specific volume of FITC-Aβ(1-40) was determined according to the method of Durchschlag and Zipper.[18] The graphical outputs were generated by GUSSI (Version 1.2.1)[19] and the final *s*-values were corrected to *s*-values in water at 20 °C ($s_{20,w}$ -values).

Surface plasmon resonance

Surface plasmon resonance (SPR) spectroscopy was performed on a Biacore T200 instrument (GE Healthcare, Uppsala, Sweden) at 298 K. N-terminally biotinylated Aβ(1-42) was immobilized on a streptavidin coated sensor chip (GE Healthcare, Uppsala, Sweden) and a concentration series of RD2D3 ranging from 0.16 to 5 µM was injected over the surface. Between each cycle, the surface was regenerated using 2 M guanidine hydrochloride. All measurements were performed in 20 mM phosphate buffer pH 7.4 including 100 mM sodium chloride. For evaluation, the response levels at the end of the association phase were plotted against the applied concentrations and fitted using the Langmuir steady state fit model implemented in the Biacore Evaluation Software 2.0 with RI = 0.

Animal experiments

In the present study 10 eight months old female homozygous tg-SwDI mice (human APP with Swedish K670N/M671L, Dutch E693Q and Iowa D694N mutations on a C57BL/6 background[20]) were used. The original mice were purchased from JAX (The Jackson Laboratory, USA) and maintain our own colony at the University of Alabama in Birmingham. Before treatment, the mice were housed 4/cage in our facility in a controlled environment (temperature 22 °C, humidity 50-60%, light from 06:00 a.m. -6:00 p.m.) with food and water available ad libitum. Following the implantation of the Alzet minipumps the mice were housed individually. The experiments were conducted according to the local Institutional Animal Care and Use Committee (IACUC) guidelines.

Behavioral tests

The mice were tested at the end of the treatment period in the following behavioral tests (open field, zero maze and Morris water maze tests).

Open field test

The open field test was performed to evaluate the on anxiety-related behavior of the treated mice. The arena (42 cm × 42 cm surrounded with clear Plexiglass sides (20 cm high)) was subdivided into two areas:

border and center. The mice were monitored with a camera driven tracker system (Ethovision XT10, Noldus, The Netherlands) for 4 min. Time spent in the border and center was analyzed. After each testing day, and in between the mice, the apparatus is wiped out with chlorhexidine and 70% ethanol and allowed to air-dry.

Zero maze

Additionally to the open field test, the zero maze was accomplished to assess the anxiety-related behavior of the mice. The maze consisted of a circular arena (65 cm diameter) that is raised 40 cm above the table. The maze was separated into four equal parts by two 15 cm high walls of opaque material and two only 0.5 cm high walls. Therefore, it consisted of two open and two closed areas. The mice were put into the circle and monitored for 4 min with a camera driven tracker system (Ethovision XT10, Noldus, The Netherlands). Analyzed was the time mice spent in the open and closed arms. After each testing day, and in between mice, the apparatus is wiped out with chlorhexidine and 70% ethanol and allowed to air-dry.

Morris Water Maze

The mice were tested for 5 days in a Morris Water Maze (MWM). The maze consisted of a blue circular tank of clear water (23 ± 1°C). The mice were placed in the water at the edge of the pool and allowed to swim in order to locate a hidden, but fixed escape platform, using extra maze cues. On day 1, the mice were placed in the pool and allowed to swim freely for 60 s to find the hidden platform (or until they find the hidden platform); each animal was tested for four trials per day. A maximum swim time per trial of 60 s was allowed; if the animal did not locate the platform in that time, it was placed upon it by the experimenter and left there for 10 s. The inter-trial interval was 120 s. Each start position (east, north, south, and west) was used equally in a pseudo random order and the animals were always placed in the water facing the wall. The platform was placed in the middle of one of the quadrants of the pool (approximately 30 cm from the side of the pool). The mouse's task throughout the experiment was to find, and escape onto the platform. The animal was monitored by Ethovision 7.1.

Statistics

All statistical calculations were performed using SigmaPlot Version 11 (Systat Software, Germany) and OriginPro8.5G. Data is represented as mean ± SEM (behavioral tests), $p > 0.05$ was considered as not significant (n.s.). Mann-Whitney Rank Sum Test was used to analyze the results of the open field test and zero maze. Escape latency to the platform within the MWM was considered as not normal distributed and therefore analyzed by Friedman Repeated Measures Analysis of Variance.

Results and Discussion

Dynamics of Aβ-polymerisation

Starting with monomeric Aβ a dynamic equilibrium is obtained that leads to virtually reversible population changes as response to external perturbations such as pressure and temperature. After a rapid

pressure jump of 40 MPa an equilibrium state is typically obtained after two to three hours at 283 K (Fig. S1). The repolymerisation at low temperatures after depolymerisation is a slow process of the order of 12 hours when enough seeds are still present in the sample. In the absence of seeds after complete depolymerization the time scale for polymerization is of the order of one week at 283 K.

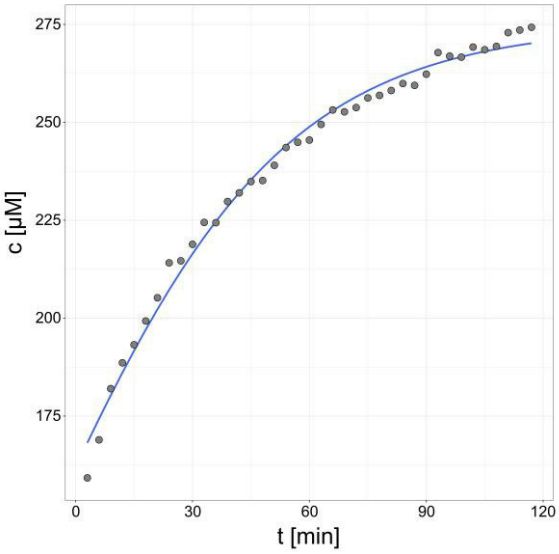

Figure S1. *Time dependent depolymerization after pressure jump.* The concentration of Aβ-monomers c_1 is plotted as a function of the time t after a pressure jump from 3 MPa to 40 MPa at 283 K. The sample contained 750 µM Aβ(1-40), 50 mM Tris-d_{11}, 90 mM NaCl, 0.5 mM EDTA-d_{16}, 1 mM NaN_3 in D_2O, pH 7.0. The data were fit by $c_1(t) = c_1(\infty) - (c_1(\infty) - c_1(0))e^{-k_- t}$ with k_- the apparent rate constant for dissociation. k_- is 0.38 10^{-3} s^{-1} with $c_1(0)$ = 157 µM and $c_1(\infty)$ = 280 µM.

Affinity of RD2D3 to Aβ monomers

Surface plasmon resonance (SPR) spectroscopy was used to determine the affinity of RD2D3 to Aβ. Biotinylated Aβ(1-42) monomers were on a streptavidin coated sensor chip (Fig. S2) at 298 K. The data can be well explained by assuming a homogeneous interaction. With this assumption the peptide binds with high affinity to Aβ with a K_D value smaller than 500 nM.

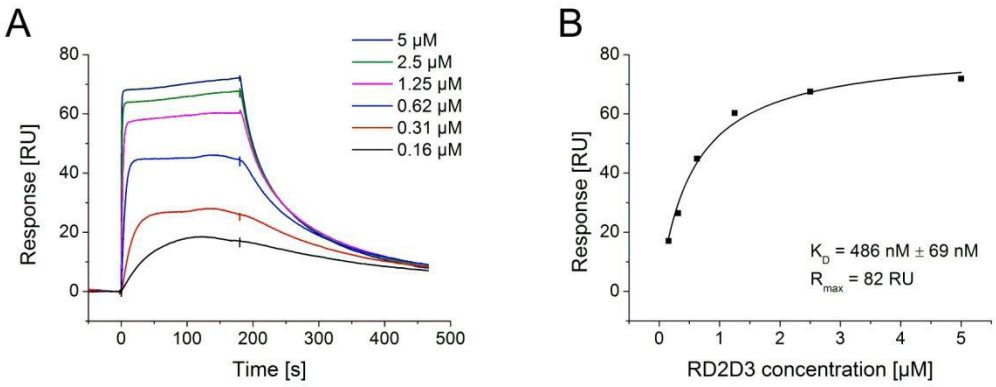

Figure S2. Affinity determination of RD2D3 to Aβ monomers. Surface plasmon resonance (SPR) spectroscopy was used to determine the affinity of RD2D3 to Aβ. Biotinylated Aβ(1-42) monomers were coupled on a streptavidin coated sensor chip and binding of the indicated RD2D3 concentrations was recorded for 180 s. (A) For evaluation, the binding responses at the end of the association phase were plotted over the RD2D3 concentrations and fitted with a steady state binding model. (B) The shown sensorgrams and fit are exemplary for four independent measurements. The K_D value is presented as mean ± σ.

Mechanism of heteropolymer formation

At higher relative concentrations of RD2 or RD2D3 the sharp NMR visible signals of Aβ become weaker and are strongly quenched. This indicates the formation of large mixed polymers with line widths too large to be observable by solution NMR spectroscopy as, in fact, they were observed by electron microscopy.[21] The reduction of the peak intensities in 1D- or 2D-spectra provides a quantitative measure for formation of these large polymers (expressed in concentrations of monomer units). In principle, monomeric free Aβ and D-peptides should be observable as well as their small complexes.

In the 1D-spectra the signals of free Aβ are characterized by relatively sharp lines that show a strong reduction of signal intensity in the presence of D-peptides. The methyl signals of Val12 and Val18 can be observed without overlap with lines of the D-peptides (Fig. 3). The concentration of the visible D-peptides can be estimated from the signals of the methylene protons H^{ε} of arginines at 3.20 ppm are best suited since Aβ contains only one arginine residue but RD2 and RD2D3 contain five and ten arginine residues, respectively. In the range between 0.8 and 1.0 ppm only the signals of methyl groups of valine, leucine and isoleucine residues are to be expected. It is dominated by the signals of Aβ(1-40) that contains six valines, two leucines and two isoleucines. RD2 and RD2D3 contain only one and two leucine residues, respectively, with methyl resonances at 0.89 ppm and 0.83 ppm (the methyl groups of two leucines in RD2D3 have nearly identical chemical shifts). At higher concentrations of the D-peptide only a broad peak remains with weak sharp signals on the top corresponding to the resonance frequencies of the free peptides (Fig. 3A, B). The broad peak presumably represents the Aβ-D-peptide complex which is also supposedly seen in [^{1}H-^{15}N]-spectra (Fig. S3). Its concentration at intermediate D-peptide concentrations can be determined by integrating this signal after subtracting the sharp signals from free Aβ and free D-peptides in the 1D-spectra.

The titration experiments were performed by mixing different quantities of two samples, a sample containing Aβ-only and a sample containing Aβ in the same concentration and a D-peptide in high concentration. This method ensured that the total Aβ concentration was constant in all experiments.

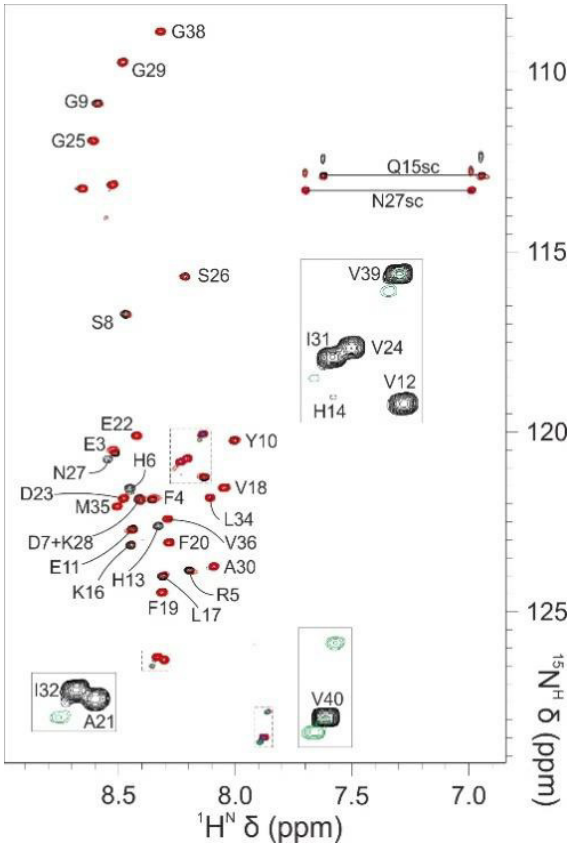

Figure S3. *Formation of Aβ heterodimers.* Superposition of [^{1}H, ^{15}N] HSQC spectra of 65 µM uniformly ^{15}N enriched Aβ in absence (black) and presence of RD2D3 with a concentration ratio 1:0.4 (red), 1:0.8 (blue) and 1:2 (green). Inserts show only 1:0 and 1:2 ratios. Temperature 283 K.

Biological effects of RD2D3

The positive biological effects of the D-enantiomeric peptides D3 and RD2 on the development of Alzheimer's disease in mice has been shown already.[21-24] For the variant RD2D3 they were not studied yet but are to be expected. We treated transgenic APPSwDI mice intraperitoneal (i.p.) for 4 weeks with 8 mg/kg/day of RD2D3 using Alzet micropumps. The Morris water maze (MWM) test (Fig. S4) is the most frequently used behavioral test of spatial learning and memory performance for rodents that relies on distal clues to navigate from start locations around the perimeter of an open swimming arena to locate a submerged escape platform. Spatial learning is assessed across repeated trials and reference memory is determined by preference for the platform area when the platform is absent.

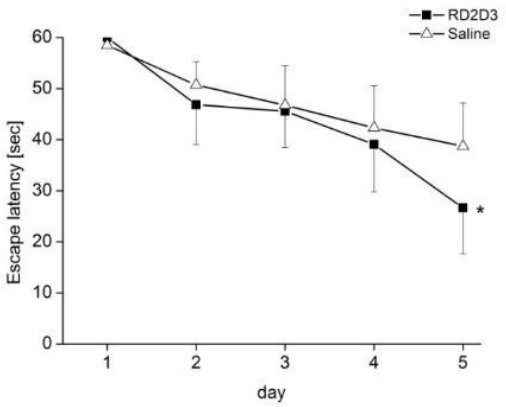

Figure S4. *Morris water maze test in transgenic mice with and without treatment with RD2D3.* Transgenic (APPSwDI) mice were treated with 8 mg/kg/day RD2D3 or saline i.p. for 4 weeks. Data is represented as mean ± standard error of mean (SEM), *p ≤ 0.05.

The intraperitoneal (i.p.) treatment of transgenic Alzheimer mice (tg-APPSwDI) with RD2D3 significantly improved the cognitive performance of the animals. Long-term memory evaluation in the Morris water maze did show significant differences between RD2D3 treated animals compared to vehicle treated tg control in escape latency (Fig. S4). The open field test provides data for the assessment of novel environment exploration and for the effects of drugs on anxiety-related behavior of mice, which can also be evaluated by zero maze. Changes in the behavior are hints for hypo- or hyperactivity. Importantly, RD2D3 had no influence on the general behavior of tg-APPSwDI mice as demonstrated by no differences in time spend in the center or open arena between saline and RD2D3 treated animals in the open field and the zero maze experiments (Fig. S5). Therefore, APPSwDI mice show no changes in general activity and fear upon RD2D3 treatment.

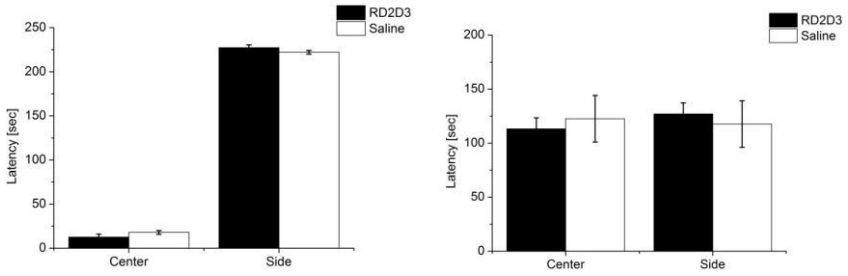

Figure S5. *Influence of RD2D3 on the behaviour of mice*. (Left) open field test, (right) zero maze test.

References

[1] W. B. Stine, K. N. Dahlgren, G. A. Krafft, M. J. LaDu, *J. Biol. Chem.* **2003**, *278*, 11612-11622.
[2] C. E. Munte, M. Beck Erlach, W. Kremer, J. Koehler, H. R. Kalbitzer, *Angew. Chem. Int. Ed.* **2013**, *52*, 8943-8947.
[3] D. S. Raiford, C. L. Fisk, E. D. Becker, *Anal. Chem.* **1979**, *51*, 2050-2051.
[4] D. S. Wishart, C. G. Bigam, J. Yao, F. Abildgaard, H. J. Dyson, E. Oldfield, J. L. Markley, B. D. Sykes, *J.Biomol. NMR* **1995**, *6*, 135-140.
[5] F. H. Schumann, H. Riepl, T. Maurer, W. Gronwald, K.-P. Neidig, H. R. Kalbitzer, *J.Biomol. NMR* **2007**, *39*, 275-289.
[6] M. R. Arnold, W. Kremer, H.-D. Lüdemann, H. R. Kalbitzer, *Biophys. Chem.* **2002**, *96*, 129-140.
[7] J. E. Tanner, *J. Chem. Phys.* **1970**, *52*, 2523-2526.
[8] G. Wider, V. Dotsch, K. Wuthrich, *J. Magn. Reson., Ser A* **1994**, *108*, 255-258.
[9] M. D. Pelta, G. A. Morris, M. J. Stchedroff, S. J. Hammond, *Magn. Reson. Chem.* **2002**, *40*.
[10] C. Wierschem, Master thesis, University of Regensburg, 2003.
[11] D. V. Laurents, P. M. Gorman, M. Guo, M. Rico, A. Chakrabartty, M. Bruix, *J. Biol. Chem.* **2005**, *280*, 3675-3685.
[12] K. Heremans, L. Smeller, *Biochim. Biophys. Acta, Protein Struct. Mol. Enzymol.* **1998**, *1386*, 353-370.
[13] F. Oosawa, *J. Theor. Biol.* **1970**, *27*, 69-86.
[14] I. K. MacGregor, A. L. Anderson, T. M. Laue, *Biophys. Chem.* **2004**, *108*, 165-185.
[15] P. Schuck, *Biophys. J.* **2000**, *78*, 1606-1619.
[16] P. Schuck, SEDFIT **2014**. Web. 22 November 2014. Available at http://www.analyticalultracentrifugation.com/default.htm
[17] T. Laue, B. Shah, T. Ridgeway, S. Pelletier, in *Analytical Ultracentrifugation in Biochemistry and Polymer Science* (Eds.: S. E. Harding, A. J. Rowe and J. C. Horton) Cambridge Royal Society of Chemistry, **1992**, 90-125.
[18] H. Durchschlag, P. Zipper, *Ultracentrifugation* **1994**, 20-39.
[19] C. A. Brautigam, *Methods Enzymol.* **2015**, *562*, 109-133.
[20] J. Davis, F. Xu, R. Deane, G. Romanov, M. L. Previti, K. Zeigler, B. V. Zlokovic, W. E. Van Nostrand, *J. Biol. Chem.* **2004**, *279*, 20296-20306.
[21] A. N. Klein, T. Ziehm, M. Tusche, J. Buitenhuis, D. Bartnik, A. Boeddrich, T. Wiglenda, E. Wanker, S. A. Funke, O. Brener, *PloS one* **2016**, *11*, e0153035.
[22] S. Aileen Funke, T. van Groen, I. Kadish, D. Bartnik, L. Nagel-Steger, O. Brener, T. Sehl, R. Batra-Safferling, C. Moriscot, G. Schoehn, *ACS Chem. Neurosci.* **2010**, *1*, 639-648.
[23] T. Van Groen, K. Wiesehan, S. A. Funke, I. Kadish, L. Nagel-Steger, D. Willbold, *ChemMedChem* **2008**, *3*, 1848-1852.
[24] O. O. Olubiyi, D. Frenzel, D. Bartnik, J. M. Gluck, O. Brener, L. Nagel-Steger, S. A. Funke, D. Willbold, B. Strodel, *Curr. Med. Chem.* **2014**, *21*, 1448-1457.

Author Contributions

I.A.C., C.E.M., M.B.E., W.K. and H.R.K. performed and evaluated the NMR experiments on Aβ. T.Za. carried out and evaluated with L.N.-S. the ultracentrifugation experiments. T.vG., I.K. and D.W. planned the animal experiments. T.vG. and I.K. performed, supervised and evaluated with J.K. the in vivo and ex vivo experiments. T.Zi. performed and evaluated the SPR experiments. H.R.K. devised the study together with D.W.. All authors read the manuscript carefully and discussed the results.